University of Massachusetts Amherst

From the SelectedWorks of Derek Lovley

2009

Novel Strategy for Three-Dimensional Real-Time Imaging of Microbial Fuel Cell Communities: Monitoring the Inhibitory Effects of Proton Accumulation Within the Anode Biofilm

Derek Lovley, *University of Massachusetts - Amherst*
Ashley E Franks
Kelly P Nevin
Hongfei Jia
Mounir Izallalen, et al.

Available at: https://works.bepress.com/derek_lovley/71/

Novel strategy for three-dimensional real-time imaging of microbial fuel cell communities: monitoring the inhibitory effects of proton accumulation within the anode biofilm

Ashley E. Franks,*[a] Kelly P. Nevin,[a] Hongfei Jia,[b] Mounir Izallalen,[a] Trevor L. Woodard[a] and Derek R. Lovley[a]

Received 19th September 2008, Accepted 13th November 2008
First published as an Advance Article on the web 1st December 2008
DOI: 10.1039/b816445b

Harvesting electricity from the environment, organic wastes, or renewable biomass with microbial fuel cells (MFCs) is an appealing strategy, but the destructive sampling required to investigate the anode-associated biofilms has hampered research designed to better understand and optimize microbe–anode interactions. Therefore, a MFC that permits real-time imaging of the anode biofilm with confocal scanning laser microscopy was developed. In this new MFC *Geobacter sulfurreducens*, an organism closely related to those often found on MFC anodes and capable of high current densities, produced current comparable to that previously reported with other MFC designs. *G. sulfurreducens* engineered to produce the fluorescent protein mcherry to facilitate real-time imaging produced current comparable to wild-type cells. Introducing C-SNARF-4, a pH-sensitive fluoroprobe, into the anode chamber revealed strong pH gradients within the anode biofilms. The pH decreased with increased proximity to the anode surface and from the exterior to the interior of biofilm pillars. Near the anode surface pH levels were as low as 6.1 compared to *ca.* 7 in the external medium. Various controls demonstrated that the proton accumulation was associated with current production. Dropping the pH of culture medium from 7 to 6 severely limited the growth of *G. sulfurreducens*. These results demonstrate that it is feasible to non-destructively monitor the activity of anode biofilms in real time and suggest that the accumulation of protons that are released from organic matter oxidation within anode biofilms can limit current production.

Introduction

Microbial fuel cells (MFCs) show promise as a strategy for harvesting electricity from the environment, wastes, and renewal biomass, but a better understanding of the factors limiting power production in MFCs is required in order to rationally optimize their many potential applications.[1–3] To date, most studies on MFCs have focused on the influence of different fuel cell architectures and/or membrane and electrode materials on MFC performance while empirically treating the microorganisms colonizing the electrodes as a 'black box'.[4] One reason for this has been the lack of methods for visualizing electrode communities or querying their activity without destructively sampling those communities.

One of the key reactions in MFC power production is the oxidation of organic matter with electron transfer to the anode, which not only initiates current flow but also provides energy for the microorganisms catalyzing this reaction.[2,5] As previously

[a]*Department of Microbiology, University of Massachusetts, Amherst, Massachusetts, 01002, USA. E-mail: mailto:aefranks@microbio.umass.edu; Fax: +1 413-545-1578; Tel: +1 413-577-2440*
[b]*Materials Research Department, Toyota Research Institute of North America, Ann Arbor, Michigan, 48105, USA*

Broader context

The direct conversion of organic wastes and biomass to electricity with microbial fuel cells offers the potential for producing high-value, carbon-neutral energy, from inexpensive source materials. However, at present, the power output of microbial fuel cells is too low for most envisioned applications. Further optimization has been stymied by a lack of understanding of the factors controlling the activity of the microorganisms that colonize the anode of microbial fuel cells and are responsible for producing the current. Here we report on a novel approach which makes it feasible to image actively metabolizing and growing cells within the anode biofilm in real time with a confocal scanning laser microscope. *G. sulfurreducens*, a well studied current-producing microorganism, was engineered to express the red fluorescent protein, mcherry. The growth of the fluorescent cells on the anode was monitored over time. When a fluorescent dye that is sensitive to pH was introduced it was possible to measure pH throughout different layers of the biofilm. During active current production, the pH deep within the biofilm dropped to levels shown to inhibit the activity of *G. sulfurreducens*. These results suggest that strategies to facilitate proton flux out of the biofilm may increase power output.

This journal is © The Royal Society of Chemistry 2009

reviewed,[2] electron transfer to anodes can be promoted with the addition of artificial electron shuttles or some microorganisms can produce their own shuttles.[6–8] However, direct electron transfer from microorganisms to the anode surface[9–11] or through a conductive anode biofilm[12–14] is expected to be the most effective mechanism for current production for most MFC applications.[2] Under these conditions the anode of the MFC serves as an extracellular electron acceptor.

The fate of protons produced from organic matter oxidation coupled to extracellular electron transfer is significantly different than during the reduction of commonly considered soluble electron acceptors, such as oxygen, nitrate, sulfate, or fumarate, that are reduced intracellularly.[15] Intracellular reduction of these electron acceptors consumes the protons that are produced during organic matter oxidation (Fig. 1a). However, when electrons are transferred to an extracellular electron acceptor, such as Fe(III) oxides or electrodes, there is a net production of protons in the cytoplasm (Fig. 1b). The resulting lower proton gradient across the inner membrane and the energetic requirement to export these protons may account for the low growth yields that result from reduction of extracellular electron acceptors.[15]

Accumulation of the protons released from extracellular electron transfer is unlikely to be a significant factor during Fe(III) oxide reduction in sedimentary environments because cell densities are generally low and the substantial environmental buffering capacity can consume the protons released into the extracellular environment during the relatively slow rates of Fe(III) reduction in these systems. In contrast, the goal for most MFCs is to have high rates of organic matter oxidation, resulting in much greater proton production. Furthermore, cell densities can be much higher in MFCs than in sediments, with substantial biofilms forming on anode surfaces in some cases.[13,16,17] Thus, there is the potential for an overall acidification of the anode medium as well as a more intense localized proton accumulation within the anode biofilm. Microorganisms growing in anode biofilms may not be well-adapted for growth within acidic biofilms zones because they are unlikely to encounter such conditions during growth on natural electrons acceptors, such as Fe(III) oxides.

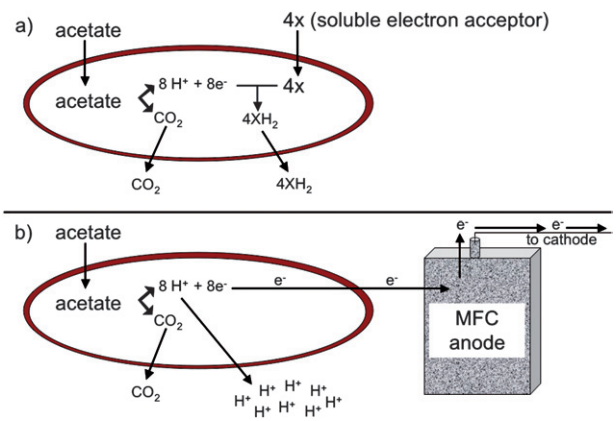

Fig. 1 Difference in proton fate between oxidation of acetate with reduction of soluble electron acceptor (a) *versus* extracellular electron transfer to an insoluble electron acceptor (b). Protons are consumed in the cytoplasm when a soluble electron acceptor, such as fumarate, is utilized whereas protons must be released from the cell during reduction of an insoluble electron acceptor, such as an electrode.

Most previous studies on the fate of protons in MFCs have been concerned with the need for effective transport from the anode to the cathode in order to prevent electrochemical limitations.[18–24] Protons must migrate from the anode to the cathode in order to maintain charge balance and to prevent acidification of the anode and alkalization of the cathode. The impact of proton accumulation on the activity of microorganisms in the anode biofilm has only recently been considered[25] and primarily on a theoretical basis.[26]

Recent modeling of proton production and flux in anode biofilms[26] focused on *G. sulfurreducens*. The functioning of this microorganism on anode surfaces is being intensively studied[9,11,14,16,17,27,28] because it is closely related to the *Geobacteraceae* that have been found to predominate on anodes harvesting current from sediments and complex wastes.[9,27,29–32] Furthermore, detailed functional studies on the physiology of this organism are feasible because of the availability of its complete genome sequence[33] and a genetic system.[34]

Modeling acetate consumption of *G. sulfurreducens* in anode biofilms indicated that accumulation of protons within the anode biofilm rather than a lack of substrate, was the factor likely to limit current production.[26] It was calculated that, if *G. sulfurreducens* became metabolically inactive at pH 6 or lower, then a substantial portion of the anode biofilm closest to the anode surface would not contribute to current production under typical buffering conditions. Increasing the concentration of phosphate buffer in a poised system in which the anode was thought to be colonized by microorganisms closely related to *G. sulfurreducens* increased current in accordance with the predictions of this model.[26]

However, these results were only qualitative and much more information will be required before it will be possible to develop models that can predict the impact of changes in MFC designs on proton flux and current output. Most importantly, the degree to which pH actually declines in anode biofilms was not determined, nor was there information on the pH levels which actually inhibit cells from contributing to current production. The structure and thickness of the biofilm was not determined[26] and *G. sulfurreducens* anode biofilms are typically not homogenous as was modeled.[26] Rather, they are typically complex structures,[13,17] which is likely to impact on proton flux out of the biofilm and thus current output. The use of a mixed community in previous studies[26] complicates the interpretation of the results because microorganisms with different pH tolerances may inhabit different microniches in the biofilm. Furthermore, the previous studies were conducted with anodes poised with a potentiostat, which may overestimate the potential for limitation by proton accumulation by removing other barriers to current production, leading to higher rates of electron donor oxidation and proton production than may be observed in a true microbial fuel cell.

Here we report on a novel microbial fuel cell system that makes it possible for the first time to visualize a live, functioning, anode biofilm in real time with confocal scanning laser microscopy. With this approach we were able to accurately measure proton accumulation specifically associated with current production and document the important role that biofilm structure has on pH gradients within the biofilm.

This journal is © The Royal Society of Chemistry 2009

Results and discussion

Real time imaging of *G. sulfurreducens* during power production in a MFC

G. sulfurreducens produced current in the MFCs modified for real-time imaging, at current densities (3.5 A m^{-2}) comparable to those previously reported in MFCs with similar materials but not modified for real-time imaging.[17] Typically a lag period of 150–200 h was followed by a quick increase in power production, with maximum power production being reached after 300 h. As previously reported,[17] once maximum production had been reached the biofilms indefinitely maintained a steady power output. Cells expressing the fluorescent protein mcherry produced current similar to wild type (Fig. 2). The growth of the cells expressing mcherry could readily be non-destructively observed in real time (Fig. 3). In a manner similar to wild-type cells in previously described MFCs, the mature biofilms of the cells expressing mcherry covered a majority of the anode surface and contained pillars structures up to 50 μm in height (Fig. 3). These results demonstrate that the modifications made to the MFC in order to make it suitable for real-time imaging did not change the basic properties of the anode biofilm.

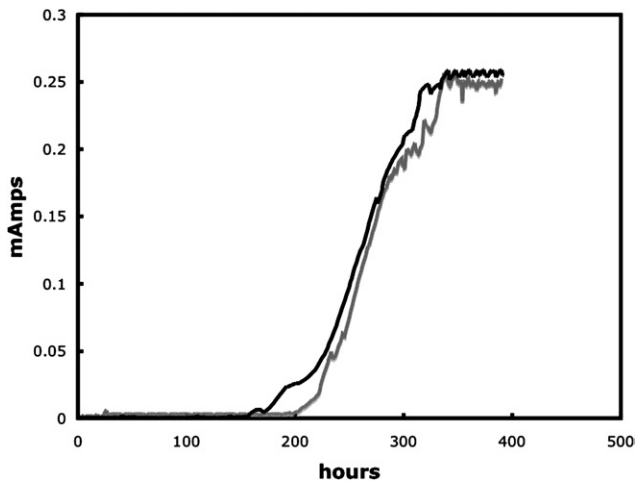

Fig. 2 Power out of wildtype *G. sulfurreducens* (black line) and *G. sulfurreducens* expressing mcherry (grey line).

Direct observation of pH gradients in current-producing biofilms

The pH within the biofilm could be measured following the introduction of C-SNARF-4 to the influent medium (Fig. 4). As expected, the pH of the external medium above and outside the biofilm was *ca.* 7. Within individual biofilm pillars there was a clear vertical pattern of decreasing pH with closer proximity to the anode surface. In the horizontal plane, pH decreased going from the outer surfaces of the pillars to the inner core. The difference in the proton concentration between the bulk fluid and the cells deep within the biofilm closest to the anode surface was almost 10-fold (*i.e.* 1 pH unit). Spaces within the biofilm had higher pH levels than within nearby dense zones of cells. The pH was lower in the low-cell density spaces within the biofilm closer to the anode surface than comparable zones at greater heights.

Disconnecting the anode from the cathode disrupted the flow of electrons, preventing the anode from accepting electrons and stopping current production in the MFC (Fig. 5a) After current, and thus proton production, were inhibited the pH gradient was measured every 15 min. Within 30 min the pH gradients previously observed (Fig. 4) during current production had dissipated, even close to the anode surface, and the pH thorough out the entire biofilm did not differ significantly from the bulk fluid (Fig. 5b). This is consistent with the expected lack of proton production in the absence of acetate oxidation coupled to electron transfer to the anode. When the anode and cathode were reconnected the MFC immediately returned to previous power levels demonstrating no detrimental effects due to the disconnection (Fig. 5a).

When *G. sulfurreducens* was grown on the anode surface material but with fumarate provided as a soluble electron acceptor and the anode not connected to the cathode, a thick, highly differentiated biofilm developed as previously reported.[29] The pH within the biofilms growing on fumarate was similar to that in the external medium both close to the base of the biofilm and at greater heights (Fig. 6). This is consistent with the fact that extracellular proton production is not expected during growth with a soluble electron acceptor such as fumarate.

These results demonstrate that there was a significant accumulation of protons within the anode biofilm and that this was related to current production. The finding that pH was lowest within the cores of the biofilm pillars and nearest the anode surface can be attributed, at least in part, to the diminished capacity for these environments to exchange with the buffer in the external medium compared with the outer surfaces of the

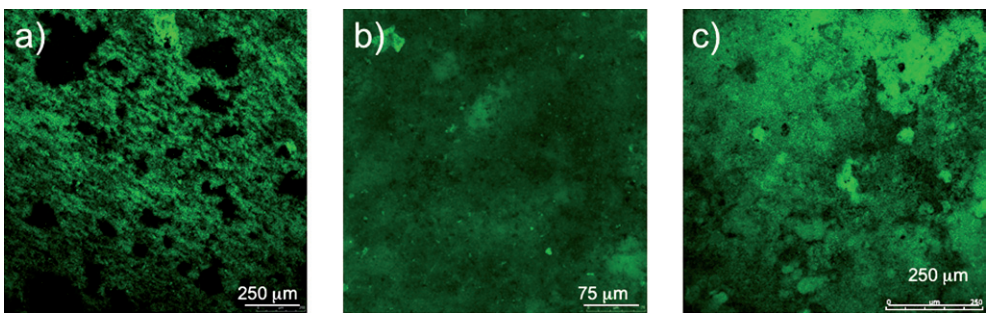

Fig. 3 Time series of biofilm development during power production. (a) Thin, single layer biofilm cells covering most of the anode surface that formed at 0.001 mA. (b) Uniform biofilm up to 30 μm in height at 0.04 mA. (c) Mature highly differentiated biofilm more than 50 μm thick at 0.21 mA.

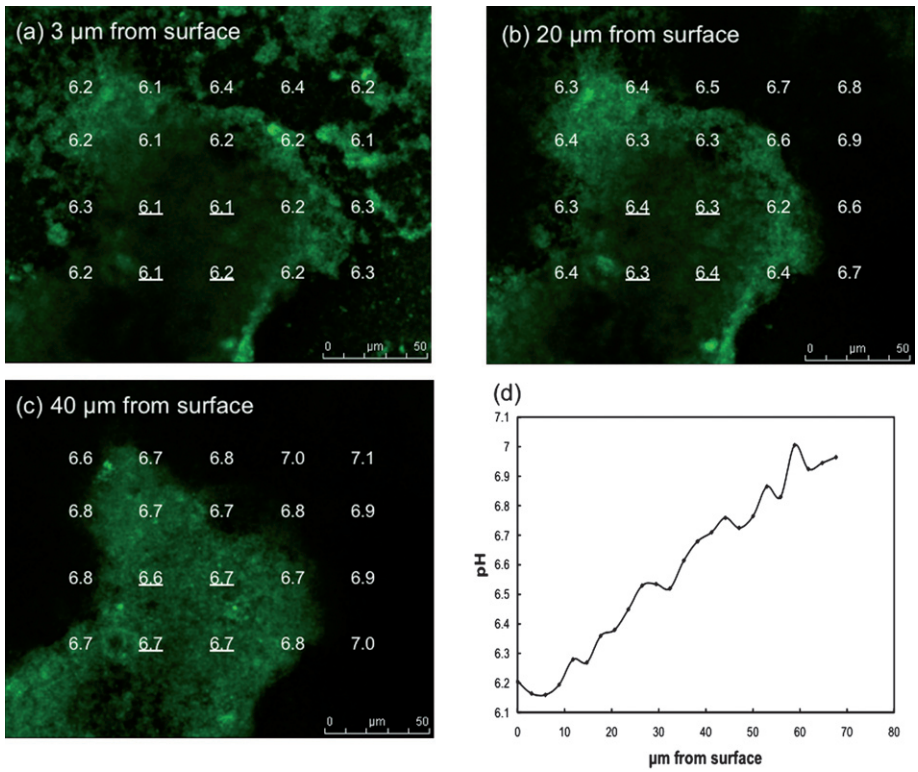

Fig. 4 pH gradients in *G. sulfurreducens* anode biofilm. (a–c) pH at different distances from anode surface and across biofilm pillar structure. (d) Average pH at the four locations within the center of the biofilm pillar underlined in a–c *versus* distance from the anode surface.

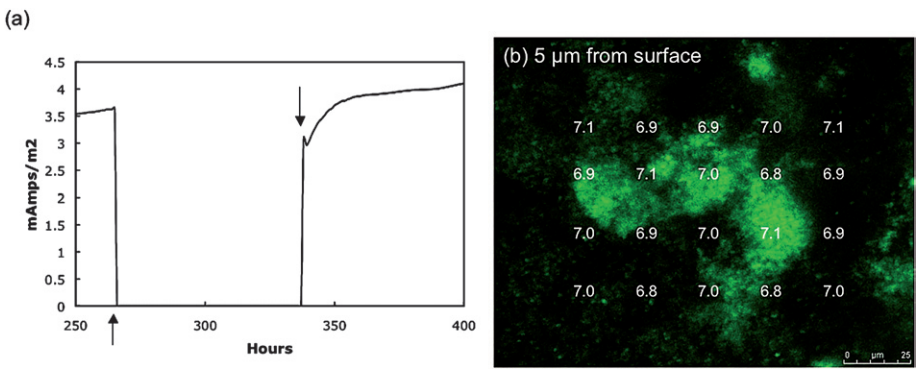

Fig. 5 Disconnected fuel cell. (a) The connection between the anode and cathode was removed (↑) preventing the anode from being an electron acceptor. Reconnecting the anode and cathode (↓) returned power production to normal almost immediately demonstrating a viable biofilm. (b) Measurements of pH 30 min after the anode and cathode had been disconnected for 30 min.

biofilm. However, an additional consideration, that cannot be ruled out with the present data, is that rates of microbial metabolism may be higher in some areas of the biofilm. For example, cells in close proximity to the anode may have higher rates of respiration because they have more ready access to the electron acceptor than cells at a distance that must rely on longer-range electron transfer which could involve greater resistances to electron flow.

Impact of pH on *G. sulfurreducens* metabolism

The pH optimum for *G. sulfurreducens* has not been previously determined. Growth with the soluble electron acceptor fumarate was significantly better at pH 7 (grow rate $0.21 \pm 01\ h^{-1}$; mean $\pm$ standard error; $n = 3$) than at pH 6 (grow rate $0.04 \pm 0.02\ h^{-1}$), suggesting that the decline in pH deep in the anode biofilms was probably sufficient to inhibit metabolism.

In order to further evaluate the effect of pH on current production anode biofilms were grown on graphite sticks in a more traditional 'H-cell' system in which the anode potential was poised with a potentiostat. With this system it was possible to readily change the pH of the bicarbonate-buffered medium simply by changing the proportion of carbon dioxide in the gas flushing the anode chamber and to continuously monitor pH in the chamber. Changing the gas phase from N_2/CO_2 (80 : 20) to CO_2 decreased the pH of the bulk medium from *ca.* 6.8 to 6.1

 This journal is © The Royal Society of Chemistry 2009

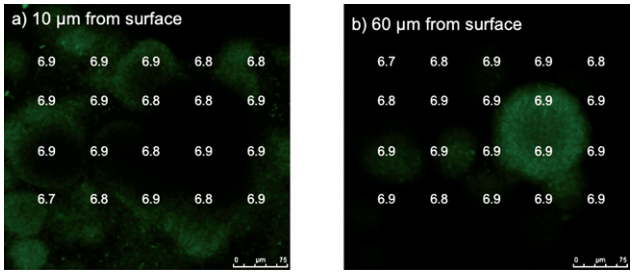

Fig. 6 pH at two distances from the graphite surface (a and b) in biofilms grown in MFC apparatus but with anode and cathode not connected and with fumarate as the electron acceptor.

(Fig. 7a). The decline in pH was associated with a precipitous drop in current. As soon as the gas phase was changed back to N_2/CO_2 (80 : 20) the pH reverted to pH 6.8 and current production rebounded, suggesting that the lower pH did not permanently damage the biofilm. These results demonstrated that low pH does inhibit the activity of the anode biofilm.

In contrast, if the gas phase was switched from N_2/CO_2 (80 : 20) to just N_2 there was an immediate increase in pH that was associated with an increase in current (Fig. 7b). When the pH was readjusted by switching to N_2/CO_2 (80 : 20) current decreased to original levels. This result is consistent with the concept that proton accumulation within anode biofilms is inhibitory and can be alleviated by increasing the sink for protons in the external medium.

Experimental

Strains and growth conditions

G. sulfurreducens strain PCA (ATCC 51573) was obtained from our laboratory collection and routinely grown under anaerobic conditions with acetate as the electron donor and fumarate as the electron acceptor as previously described.[34] Spectomycin was added at a final concentration of 250 μg ml^{-1} when required for plasmid selection. In order to fluorescently label cells for monitoring with confocal scanning laser microscopy (CSLM) the gene for the fluorescent protein, mcherry,[35] was amplified with the primer pair Mchr_F: GCAGAATTCGAATTCAGGAGGATCCATATG and Mchr_R: GCAGGATCCCTAGACTCGAGAAGCTTA and cloned into the *EcoR*I-*BamH*I site of expression plasmid pRG5[36] to form the plasmid pRG5Mc. pRG5Mc was electroporated into *G. sulfurreducens* as previously described.[34]

System for real-time imaging of anode biofilms

The previously described[17] 'mini-stack' microbial fuel cells were modified to position the graphite anode within CSLM imaging distance (Fig. 8). The entire media flow was diverted across the anode (0.81 cm^2 size) through a channel (0.5 mm deep and 6.35 mm wide) that was comprised of a coverslip on the side opposite the anode. The modified system was 1/3 thinner than the original mini-stack, making it possible to position the entire MFC on the microscope stage without disruption to the fuel cell set up. To avoid cathodic limitations the anode was 1/8 the size of the cathode. A 560 Ohm resistor provided load between the anode and cathode.

Cells were inoculated into the fuel cell as previously described[17] and once growth started acetate-containing medium was continuously pumped through the anode chamber at a flow rate

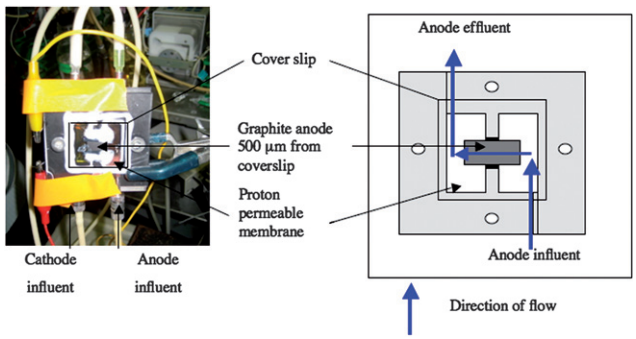

Fig. 8 Microbial fuel cell modified from 'mini-stack' design[17] to allow nondestructive real-time imaging. Flow (blue arrows) was diverted across a 0.81 cm^2 graphite anode (grey area). A 0.5 mm deep and 6.35 mm wide channel was formed with onside being formed by a cover slip to allow imaging with confocal scanning laser microscopy.

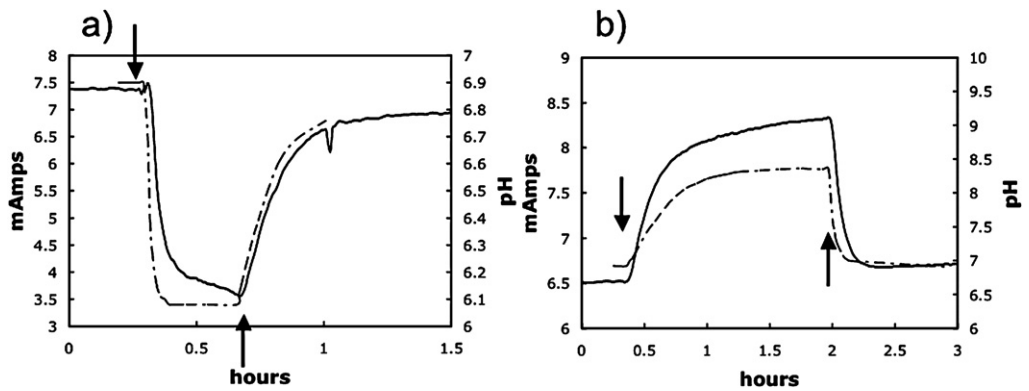

Fig. 7 Representative examples of decrease and increase in power production due to an decrease or increase in pH of bulk fluid. Where indicated (↓) the gas phase in the anode chamber was switched from N_2/CO_2 to either CO_2 only resulting a decrease in pH (a) or N_2 only resulting in a rise in pH (b). When gassing was returned to the normal N_2/CO_2 (80 : 20) mix (↑), the pH returned to ~6.9 and power production returned to levels comparable to those before the gassing was changed.

of 0.1 ml min^{-1}. A Keithley datalogger (Model 2700 DMM, Keithly Instruments Inc, Ohio, USA) connected to a computer running Excelink was used to monitor the voltage across the 560 Ohm resistor of the fuel cell. In order to grow biofilms on the anode material without current production the anode and cathode were disconnected and fumarate (40 mM) was provided as the electron acceptor.

Measuring pH within anode biofilms

C-SNARF-4 (seminaphthorhodafluor-4F 5-(and-6) carboxylic acid; Molecular Probes), a pH-sensitive fluoroprobe, has been shown to be a reliable indicator of pH within microbial biofilm microenvironments when coupled with quantitative CSLM imaging.[37] For calibration, SNARF-4 standards (1 μm final concentration) were made in freshwater medium at pH ranges from 5 to 7.5. The anode chamber was filled with these standards, the medium was excited at 488 nm and the emission ratio of 640 to 580 nm for each standard was determined using a Leica TCS SP5 microscope with a HCX APO 63x (NA 0.9) objective at various depths with image analysis conducted with Leica LAS AF software (Leica Microsystems GmbH, Wetzlar, Germany) to calculate a standard curve as previously described.[37]

In order to evaluate pH within biofilms the medium flowing into the anode chamber was amended with C-SNARF-4 (1 μm) and biofilms where immediately imaged in consecutive line scans with excitation at 588 nm to detect the mcherry fluorescence and 488 nm for pH analysis. Areas to be imaged where chosen at random and image stacks where analyzed in the *xyz* planes. Regions of interest comprising an area of 80 μm^2 where analyzed through the biofilm at regular intervals in the *x*, *y* and *z* axes. Biofilms grown with the anode as the electron acceptor were examined when current reached 2.2 mA whereas biofilms grown with fumarate as the electron acceptor were examined when the biofilm was visible by eye.

Effect of pH on current production

In order to evaluate the effect of pH on current production *G. sulfurreducens* biofilms were grown on graphite stick electrodes with acetate as the electron donor as previously described[13] with a continuous medium flow at a dilution rate of 0.15 h^{-1}. The anode was poised at +300 mV *versus* Ag/AgCl. In order to lower the pH of the medium the gas phase was changed from N_2/CO_2 (80 : 20), which maintains the bicarbonate-buffered medium at *ca.* 7, to all CO_2. The pH was increased by changing the gas phase to all N_2. Changes in pH were monitored with a pH probe (Corning) inserted into the anode chamber.

Conclusions

The MFC described here is, to our knowledge, the first system that permits real-time, three-dimensional imaging of functioning anode biofilms. Anode biofilms have previously been documented with techniques such as scanning electron microscopy;[9,20,38] epiflourescent microscopy[10,39] or confocal scanning laser microscopy,[17,40–42] but these procedures required removing the anode from the MFC with the resulting loss of viability. The method described here makes it possible not only to watch cells grow and form the anode biofilm but also to document their activity throughout the biofilm. The C-SNARF-4 reagent is just one of many possible fluorescent reporters that might be used to document chemical gradients or microbial activity within anode biofilms in response to different environmental conditions that may be imposed to influence MFC outputs. Real-time imaging is also likely to be essential for elucidating the interactions between the diverse microbial species that may simultaneously colonize MFC anodes or cathodes.

Here we have shown how the real-time imaging approach can be applied to resolving an important issue in MFC research, the possibility of proton accumulation with anode biofilms, which previously could only be addressed in an indirect manner. The results clearly demonstrate proton accumulation at levels likely to inhibit current production. The patterns of proton accumulation suggest that the complex pillared structure of *G. sulfurreducens* anode biofilms may play an important role in dissipating proton accumulation compared to what would be expected for a more homogenous biofilm that did not have spaces to facilitate buffer influx and proton efflux.

The results suggest that modifications to the structure and/or materials of MFCs to promote proton flux out of anode biofilms or engineering cells to form more porous biofilms or better tolerate lower pH might improve current output of MFCs. The novel approach described here is expected to be an important tool in evaluating these and other potential MFC modifications.

Acknowledgements

This research was supported by the Office of Naval Research Award No. N00014-07-1-0966, Toyota Technical Center, and the Office of Science (BER) and US Department of Energy Cooperative Agreement No. DE-FC02-02ER63446.

References

1 B. E. Logan and J. M. Regan, *Environ. Sci. Technol.*, 2006, **40**, 5172–5180.
2 D. R. Lovley, *Nat. Rev. Microbiol.*, 2006, **4**, 497–508.
3 Z. Du, H. Li and T. Gu, *Biotechnol. Adv.*, 2007, **25**, 464–482.
4 V. G. Debabov, *Mikrobiologiya*, 2008, **77**, 149–157.
5 D. R. Lovley, *Curr. Opin. Biotechnol.*, 2006, **17**, 327–332.
6 M. Lanthier, K. B. Gregory and D. R. Lovley, *FEMS Microbiol. Lett.*, 2008, **278**, 29–35.
7 E. Marsili, D. B. Baron, I. D. Shikhare, D. Coursolle, J. A. Gralnick and D. R. Bond, *Proc. Natl. Acad. Sci. U. S. A.*, 2008, **105**, 3968–3973.
8 T. H. Pham, N. Boon, P. Aelterman, P. Clauwaert, L. De Schamphelaire, L. Vanhaecke, K. De Maeyer, M. Hofte, W. Verstraete and K. Rabaey, *Appl. Microbiol. Biotechnol.*, 2008, **77**, 1119–1129.
9 D. R. Bond and D. R. Lovley, *Appl. Environ. Microbiol.*, 2003, **69**, 1548–1555.
10 S. K. Chaudhuri and D. R. Lovley, *Nat. Biotechnol.*, 2003, **21**, 1229–1232.
11 D. E. Holmes, S. K. Chaudhuri, K. P. Nevin, T. Mehta, B. A. Methe, A. Liu, J. E. Ward, T. L. Woodard, J. Webster and D. R. Lovley, *Environ. Microbiol.*, 2006, **8**, 1805–1815.
12 A. Kato Marcus, C. I. Torres and B. E. Rittmann, *Biotechnol. Bioeng.*, 2007, **98**, 1171–1182.
13 G. Reguera, K. P. Nevin, J. S. Nicoll, S. F. Covalla, T. L. Woodard and D. R. Lovley, *Appl. Environ. Microbiol.*, 2006, **72**, 7345–7348.
14 N. Malvankar, K. P. Nevin, S. F. Covalla, J. P. Johnson, A. E. Franks, V. M. Rotello, M. T. Tuominen and D. R. Lovley, *Microbial Biotech.*, submitted.

 This journal is © The Royal Society of Chemistry 2009

15 R. Mahadevan, D. R. Bond, J. E. Butler, A. Esteve-Nunez, M. V. Coppi, B. O. Palsson, C. H. Schilling and D. R. Lovley, *Appl. Environ. Microbiol.*, 2006, **72**, 1558–1568.
16 K. P. Nevin, B.-C. Kim, R. H. Glaven, J. P. Johnson, T. L. Woodard, B. A. Methé, R. J. DiDonato Jr, S. F. Covalla, A. E. Franks, A. Liu and D. R. Lovley, *Microbiology*, submitted.
17 K. P. Nevin, H. Richter, S. F. Covalla, J. P. Johnson, T. L. Woodard, H. Jia, M. Zhang and D. R. Lovley, *Environ. Microbiol.*, 2008, **10**, 2505–2514.
18 G.-C. Gil, I.-S. Chang, B. H. Kim, M. Kim, J.-K. Jang, H. S. Park and H. J. Kim, *Biosens. Bioelectron.*, 2003, **18**, 327–334.
19 S. E. Oh and B. E. Logan, *Appl. Microbiol. Biotechnol.*, 2006, **70**, 162–169.
20 R. A. Rozendal, H. V. Hamelers, R. J. Molenkamp and C. J. Buisman, *Water Res.*, 2007, **41**, 1984–1994.
21 K. Rabaey, G. Lissens, S. D. Siciliano and W. Verstraete, *Biotechnol. Lett.*, 2003, **25**, 1531–1535.
22 B. Min, J. Kim, S. Oh, J. M. Regan and B. E. Logan, *Water Res.*, 2005, **39**, 4961–4968.
23 H. Liu, S. A. Cheng and B. E. Logan, *Environ. Sci. Technol.*, 2005, **39**, 5488–5493.
24 M. Grzebyk and G. Pozniak, *Sep. Purif. Technol.*, 2005, **41**, 321–328.
25 B. H. Kim, I. S. Chang and G. M. Gadd, *Appl. Microbiol. Biotechnol.*, 2007, **76**, 485–494.
26 C. I. Torres, A. Kato Marcus and B. E. Rittmann, *Biotechnol. Bioeng.*, 2008, **100**, 872–881.
27 D. E. Holmes, D. R. Bond, R. A. O'Neil, C. E. Reimers, L. R. Tender and D. R. Lovley, *Microbiol. Ecol.*, 2004, **48**, 178–190.
28 D. E. Holmes, K. P. Nevin, R. A. O'Neil, J. E. Ward, L. Adams, T. L. Woodard, H. A. Vrionis and D. R. Lovley, *Appl. Environ. Microbiol.*, 2005, **71**, 6870–6877.
29 H. S. Lee, P. Parameswaran, A. Kato-Marcus, C. I. Torres and B. E. Rittmann, *Water Res.*, 2008, **42**, 1501–1510.
30 S. Jung and J. M. Regan, *Appl. Microbiol. Biotechnol.*, 2007, **77**, 393–402.
31 Z.-D. Liu and H.-R. Li, *Biochem. Eng. J.*, 2007, **36**, 209–214.
32 L. M. Tender, C. E. Reimers, H. A. Stecher, D. E. Holmes, D. R. Bond, D. A. Lowy, K. Pilobello, S. J. Fertig and D. R. Lovley, *Nat. Biotechnol.*, 2002, **20**, 821–825.
33 B. A. Methé, K. E. Nelson, J. A. Eisen, I. T. Paulsen, W. Nelson, J. F. Heidelberg, D. Wu, M. Wu, N. Ward, M. J. Beanan, R. J. Dodson, R. Madupu, L. M. Brinkac, S. C. Daugherty, R. T. DeBoy, A. S. Durkin, M. Gwinn, J. F. Kolonay, S. A. Sullivan, D. H. Haft, J. Selengut, T. M. Davidsen, N. Zafar, O. White, B. Tran, C. Romero, H. A. Forberger, J. Weidman, H. Khouri, T. V. Feldblyum, T. R. Utterback, S. E. Van Aken, D. R. Lovley and C. M. Fraser, *Science*, 2003, **302**, 1967–1969.
34 M. V. Coppi, C. Leang, S. J. Sandler and D. R. Lovley, *Appl. Environ. Microbiol.*, 2001, **67**, 3180–3187.
35 N. C. Shaner, R. E. Campbell, P. A. Steinbach, B. N. G. Giepmans, A. E. Palmer and R. Y. Tsien, *Nat. Biotechnol.*, 2004, **22**, 1567–1572.
36 B. C. Kim, C. Leang, Y. H. Ding, R. H. Glaven, M. V. Coppi and D. R. Lovley, *J. Bacteriol.*, 2005, **187**, 4505–4513.
37 R. C. Hunter and T. J. Beveridge, *Appl. Environ. Microbiol.*, 2005, **71**, 2501–2510.
38 D. R. Bond and D. R. Lovley, *Appl. Environ. Microbiol.*, 2005, **71**, 2186–2189.
39 S. Parot, M. L. Delia and A. Bergel, *Bioresour. Technol.*, 2008, **99**, 4809–4816.
40 B. H. Kim, H. S. Park, H. J. Kim, G. T. Kim, I. S. Chang, J. Lee and N. T. Phung, *Appl. Environ. Microbiol.*, 2004, **63**, 672–681.
41 G. Reguera, R. B. Pollina, J. S. Nicoll and D. R. Lovley, *J. Bacteriol.*, 2007, **189**, 2125–2127.
42 H. Richter, K. P. Nevin*, H. Jia, D. A. Lowy, D. R. Lovley, and L. M. Tender, *Energy Environ. Sci.* submitted.